Hindawi
Mathematical Problems in Engineering
Volume 2022, Article ID 3997081, 13 pages
https://doi.org/10.1155/2022/3997081

Research Article

Research on Identification Algorithm of Cascade Control System

Damin Ding,[1,2] **Yagang Wang**,[1,2] **Wei Zhang**,[1] **and Wei Chu**[1,2]

[1]*School of Optical-Electrical and Computer Engineering, University of Shanghai for Science and Technology, Shanghai 200093, China*
[2]*Rehabilitation Engineering and Technology Institute, University of Shanghai for Science and Technology, Shanghai 200093, China*

Correspondence should be addressed to Yagang Wang; ygwang@usst.edu.cn

Received 4 June 2022; Revised 25 July 2022; Accepted 26 September 2022; Published 24 November 2022

Academic Editor: Ricardo Aguilar-Lopez

Copyright © 2022 Damin Ding et al. This is an open access article distributed under the Creative Commons Attribution License, which permits unrestricted use, distribution, and reproduction in any medium, provided the original work is properly cited.

Aiming at the problem of object model identification of modern industrial process control systems, a new closed-loop moment parameter identification online method based on the data of normal operation of the running system is proposed. In this method, only one step response data of the system is required, and appropriate convergence factors are introduced into the Laplace formula, the trapezoidal integral method is used to calculate the values of two derivatives of the transfer function, then the four unknown parameters of the second-order model can be solved by fitting the data with the least square method, and the target model can be identified. Finally, the simulation results of building different objects through Matlab show that the identification method has general applicability and good robustness with high recognition, and it is not sensitive to noise signals.

1. Introduction

In the actual industrial production environment, the internal structure of the object model is always equal to a black box. We do not know the internal structure, and it is not simple to restore the internal modeling to get an accurate model. The idea of system identification is to obtain a model equivalent to the internal model.

Arif et al. provided a thorough survey on the academic research progress and industry practices and highlighted existing issues and new trends in load modeling [1]. Podvalny and Vasiljev offered the stage-by-stage composition and identification of the non-linear model parameters that are based on the principles of a multi-alternative structure and functioning of composite systems, i.e., multi-levelness, modularity, and separation of functions, and that method can overcome the basic restrictions caused by incommutativity of non-linear and linear nodes of a system [2]. A non-linear cascaded system identification approach is presented in [3] to predict the model structure parameters that minimize the difference between the estimated and measured data, using benchmark datasets. Zhang et al. proposed an effective control loop performance assessment (CPA) of a cascade control system for many non-Gaussian distributions even the unknown mixture disturbance noise [4]. Kien and Anh proposed a new cascade training multi-layer fuzzy logic identifying the forward model of double-coupled tank system based on experiment [5]. Mavkov et al. introduced a neural network architecture, called integrated neural network (INN), for the identification of non-linear continuous-time dynamical models in state-space representation [6]. Kien et al. proposed a new cascade training multi-layer fuzzy logic for identifying forward model of multiple-input multiple-output (MIMO) non-linear double-coupled fluid tank system based on experiment platform [7], and the cascade training using optimization algorithms optimally trained multi-layer fuzzy model one by one. All parameters of the multi-layer fuzzy model were optimally and comparatively identified using DE, GA, and PSO algorithms. Khorasani and Weyer [8] extended the SPS approach to EIV systems to construct a confidence region for a single module in a simple cascade network by incorporating additional data and taking advantage of the cascade structure without estimating other modules in the network. Vörös [9] used three-block cascade models with non-linear static, linear dynamic, and non-linear dynamic

blocks to deal with the recursive identification of time-varying non-linear dynamic systems. Mattsson et al. proposed an identification method that uses a likelihood-based methodology that adaptively penalizes model complexity and directly leads to a computationally efficient implementation [10]. A hybrid backtracking search algorithm with wavelet mutation (BSA-WM) has been applied for the identification of the parameters associated with a non-linear three-stage cascaded Wiener–Hammerstein (W-H) system with polynomial non-linearities of different order [11]. Karachalios et al. [12] presented an algorithm for data-driven identification of non-linear cascaded systems with Hammerstein structure relying on the Loewner framework (LF). Vörös [13] presented a new approach to the parameter identification of non-linear dynamic systems using cascade models with non-linear dynamic, linear dynamic, and non-linear static blocks based on a least-squares iterative technique. Most of the system identification algorithms given in these studies are offline system identification based on the acquired data [14–16]. When encountering an unfamiliar controlled object system, these system identification algorithms require the controlled object to be shut down or out of the production process and stimulated with a step input signal more than once. The data generated by the controlled object are used for system identification. In engineering applications, we often encounter situations where we need to adjust the parameters of an unfamiliar controlled object. Sometimes, we do not have enough time and financial resources to obtain response data through multiple trials.

The specific categories of model identification methods can be divided into the identification of target objects through the FOPDT (first-order plus dead time) model and the SOPDT (second-order plus dead time) model. It is often necessary to rely on some methods of minimizing the error criterion. We use the least-squares method, which is relatively mature, has fewer iterations, and has better robustness. In addition to the least-squares method, there are Newton iteration method, particle swarm method, auxiliary variable method, etc. [17–19], but the above methods have different defects and are not suitable for practical applications. For example, Newton's iteration method [20, 21], duelist algorithm [22], bargaining game theory-based approach [23], biquad filters [24], and other similar algorithms [25] are too computationally expensive, particle swarm method iterations are too many, and so on. Normally, system identification is for the identification of a closed-loop system in an open-loop situation. However, in some cases, the closed-loop system does not allow the feedback loop to be disconnected [26].

Some recent studies such as Aljamaan et al. [3], Kien et al. [5, 7], Vörös [9], Mattsson et al. [10], and so on used the offline system response data that have been obtained for system identification. And these earlier studies of system identification have been improved by Li et al. [27], Liu and Gao [28] and Wang et al. [29]. Branko [30], Nino et al. [31], and Chao et al. [32]'s methods seem to be suitable for only a few scenarios and are not suitable for generalizing to other areas.

Aiming at these problems, a closed-loop moment identification method based on the data of the normal operation of the online system is proposed.

The contributions of this paper can be summarized as follows:

(1) A new closed-loop moment parameter identification online method based on the data of normal operation of the running system is proposed, which only needs to obtain the normal operating data of the system setting value change once.

(2) We introduce a suitable convergence factor λ into the Laplace formula as the best parameter to make the signal converge quickly.

(3) We propose a method of trapezoidal integration to calculate the value of the two derivations of the transfer function to solve the four unknown parameters of the second-order model by the least-squares method.

This paper selects different types of controlled objects for step response simulation, such as simple control system, non-minimum phase control system, and cascade control system. According to the analysis of input and output signals, the transfer function in the frequency domain is differentiated, and the signal data are processed by trapezoidal integration. According to the algorithm in this paper, the relevant parameters of the transfer function model can be obtained. Judge the degree of fit between the identification model and the original model through the model's Nyquist graph and the output error value.

The rest of this paper is organized as follows. Section 1 provides the cascade control system signal analysis, and object model identification is presented in Section 2. The simulations and evaluations are presented in Section 3. Finally, we present our conclusion in Section 5.

2. Signal Analysis

The magnetic heating stirrer is a laboratory instrument used for liquid mixing, mainly for heating and stirring low viscosity liquids or solid-liquid mixtures. The basic principle of this stirrer is that the magnetic field repels and attracts opposites. It drives the magnetic stirrer placed in the vessel to operate in a circular motion by changing the magnetic field, thus achieving the purpose of stirring the liquid. There are many types of magnetic stirrers. In addition to the stirring function, it also has additional functions such as heating temperature control and timing. The main types are magnetic stirrer, magnetic heating stirrer, and constant temperature heating stirrer. It has a heating temperature control system, which can heat and control the sample temperature according to the specific experimental requirements, maintain the temperature conditions required for the experimental conditions, and ensure that the liquid mixing meets the experimental requirements.

The goal of this paper is to convert the system shown in Figure 1 into an accurate mathematical model, thus facilitating the tuning of the controller. The system shown in

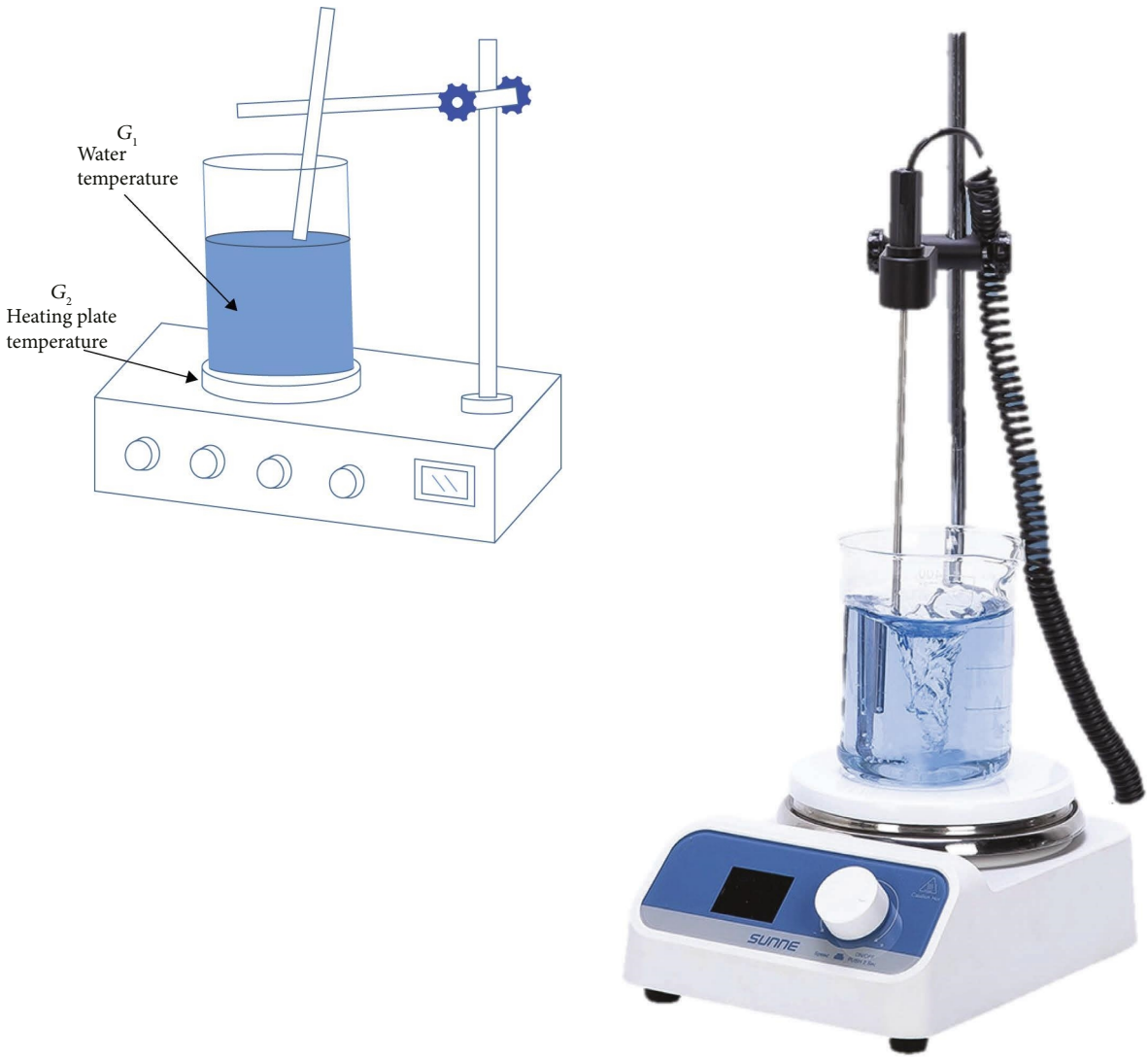

(a) (b)

Figure 1: A typical stirrer with heating function. (a) Schematic diagram. (b) Real photos.

Figure 1 is separated into internal and external loops, and the system models are identified separately based on normal operation data.

Since the internal loop is usually a non-minimum phase system, we need to verify the applicability of the method in this paper to the non-minimum phase system first and then to the overall cascade system.

In this paper, the temperature is considered the controlled variable. In this system as shown in Figure 1, the internal heater temperature is considered as the original signal, i.e., the desired value. The heater tray temperature is considered as the internal loop $G2$ output value and the water temperature is considered as the external loop $G1$ output value. The heater acts on the system tray, and the signal from the tray temperature sensor is treated as the internal loop output, which is treated as the external loop input, and the actual water temperature is treated as the external loop output so that it can be identified and converted into the mathematical model problem shown in Figure 2 in this paper.

The model of the stirrer is shown in Figure 2, where $u(s)$ is the input signal, $e_{\text{ext}}(s)$ is the outer loop noise, and $e_{\text{int}}(s)$ is the inner loop noise. A convergence factor is introduced here to avoid the integrand function not being able to be integrated, and it can converge the response signal after the signal reaches a steady state.

3. Object Model Identification

3.1. Identification Method Based on the Non-Minimum Phase Systems. A non-minimum phase system refers to a controlled object whose object transfer function has zeros, poles, or a time-delay process on the right half of the complex plane. Such systems with non-minimum phase objects are

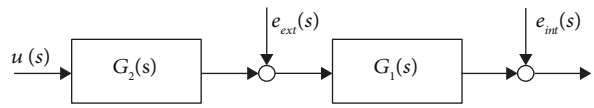

Figure 2: Mathematical model of the plant. The heater acts on the system tray, and the signal from the tray temperature sensor is treated as the internal loop output, which is treated as the external loop input, and the actual water temperature is treated as the external loop output so that it can be identified and converted into the mathematical model problem.

widely used in chemical industry reaction process controllers, power electronic converters, automatic underwater navigation controllers, and so on. Among the many types, the non-minimum phase object with the right half complex plane zero and the time-delay link is the most typical. When the controlled object has the above characteristics at the same time, it is a considerable challenge for the overall system tuning and control. Therefore, it is particularly important to be able to accurately identify the target object model.

In the actual industrial control object, due to the complexity of its order, it is more difficult to design the controller. Therefore, a second-order model with a non-minimum phase is proposed to fit and approximate the actual target system. Its form is as follows:

$$G(S) = \frac{k - s}{as^2 + bs + c} e^{-Ls}. \tag{1}$$

Put $s = j\omega$ into (1):

$$|G(j\omega)| * \arg[G(j\omega)] = \frac{k - j\omega}{a(j\omega)^2 + b(j\omega) + c} e^{-Lj\omega}. \tag{2}$$

Split (2) into amplitude and phase, as follows:

$$|G(j\omega)|^2 \left(\left(c - a\omega^2 \right)^2 + b^2 \right) = k^2 + \omega^2, \tag{3}$$

$$\omega L = -\arg[G(j\omega)] - \tan^{-1}\left(\frac{\omega}{k}\right) - \tan^{-1}\left(\frac{b\omega}{c - a\omega^2}\right). \tag{4}$$

When the frequency value takes different values, both (3) and (4) are written in the form of matrix multiplication:

$$Ax = B, \tag{5}$$

$$\frac{c^2}{k^2}|G(j\omega)|^2 + \frac{\left(b^2 - 2ac\right)}{k^2}\omega^2|G(j\omega)|^2 + \frac{a^2}{k^2}\omega^4|G(j\omega)|^2 - \frac{1}{k^2}\omega^2 = 1, \tag{6}$$

$$x = \begin{bmatrix} x_1 \\ x_2 \\ x_3 \\ x_4 \end{bmatrix} = \begin{bmatrix} \dfrac{c^2}{k^2} \\ \dfrac{b^2 - 2ac}{k^2} \\ \dfrac{a^2}{k^2} \\ \dfrac{1}{k^2} \end{bmatrix}, \tag{7}$$

$$B = \begin{bmatrix} 1 & 1 & 1 & \dots & 1 \end{bmatrix}^T. \tag{8}$$

x in equation (11) can be obtained by using the least-squares method to solve, and the unknown parameter is obtained by further solving:

$$x = \left(A^T \cdot A\right)^{-1} \cdot A^T \cdot B, \tag{9}$$

$$\begin{bmatrix} k \\ a \\ b \\ c \end{bmatrix} = \begin{bmatrix} \sqrt{\dfrac{1}{x_4}} \\ \sqrt{\dfrac{x_2 + 2\sqrt{x_1 x_3}}{x_4}} \\ \sqrt{\dfrac{x_1}{x_4}} \end{bmatrix}. \tag{10}$$

3.2. Identification Method Based on the Industrial Cascade System. As shown in the cascade control system shown in Figure 3, $SP1$ is the target value set by the user, $PV2$ is the output value of the internal loop object $G2$, $PV1$ is the output value of the external loop object $G1$, $CO2$ is the internal loop PID controller $GC2$ output value, and $SP2$ is the output of external loop PID controller $GC1$. $G1$ and $G2$ are the transfer functions of the internal and external ring objects that need to be identified, respectively.

In the cascade system, two models require model identification, namely, $G1$ and $G2$. By setting the input value of $SP1$, the input and output data of the two object models are obtained, respectively, and the data can be obtained by dividing by the Laplace transform. Equation (16) is a simplified expression for the cascading system. The detailed derivation process of this identification method will be described below.

$$G_1(s) = \frac{PV_1(s)}{CO_1(s)}, \tag{11}$$

$$G_2(s) = \frac{PV_2(s)}{CO_2(s)}. \tag{12}$$

In this section, the second-order hysteresis model is used to identify the internal and external objects in the cascade control system, and simulation verification is given. The results show that the method has good accuracy.

The model of this paper is

$$G(s) = \frac{q}{as^2 + bs + 1} e^{-Ls}. \tag{13}$$

By collecting the signals at both ends of the internal loop and external loop of the cascade control system, the calculation formula is

$$Y(s) = \int_0^\infty y(t) e^{-st} \mathrm{d}t, \tag{14}$$

$$R(s) = \int_0^\infty r(t) e^{-st} \mathrm{d}t. \tag{15}$$

Calculating the n-th order derivative on both ends of (14) and (15), (16) and (17) are obtained:

$$Y^{(n)}(s) = (-1)^{(n)} \int_0^\infty t^n e^{-st} y(t) \mathrm{d}t, \tag{16}$$

$$R^{(n)}(s) = (-1)^{(n)} \int_0^\infty t^n e^{-st} r(t) \mathrm{d}t. \tag{17}$$

The transfer function is transformed to the following formulas for the first and second order derivatives:

$$Y'(s) = G'(s)R(s) + G(s)R'(s), \tag{18}$$

$$Y''(s) = G''(s)R(s) + 2G'(s)R'(s) + G(s)R''(s). \tag{19}$$

Transform and bring convergence factor λ into (20) and (21):

$$G'(\lambda) = \frac{Y'(\lambda) - G(\lambda)R'(\lambda)}{R(\lambda)}, \tag{20}$$

$$G''(\lambda) = \frac{Y'(\lambda) - 2G'(\lambda)R'(\lambda) - G(\lambda)R''(\lambda)}{R(\lambda)}. \tag{21}$$

In (20) and (21), $G(\lambda)$, $G'(\lambda)$, and $G''(\lambda)$ are all obtained by obtaining the data trapezoidal integral (19) of the response of the object. In order to reduce the amount of calculation, take the logarithm of both ends of equation (25) to get

$$\ln G(s) = \ln q - \ln\left(as^2 + bs + 1\right) - Ls. \tag{22}$$

Take the derivative of the two ends of (20) twice and denote it as $J_1(s)$ and $J_2(s)$.

$$\frac{G'(s)}{G(s)} = -\frac{2as + b}{as^2 + bs + 1} - L \Leftrightarrow J_1(s), \tag{23}$$

$$\frac{G''(s)G(s) - G^2(s)}{G^2(s)} = \frac{2a^2s^2 + b^2 + 2abs - 2a}{\left(as^2 + bs + 1\right)^2} \Leftrightarrow J_2(s). \tag{24}$$

Transform (23) and bring $s = \lambda$ into the following :

$$\begin{aligned} J_2(\lambda) = {} & \left(-2\lambda^2 J_2(\lambda) - 2\right)a - 2\lambda J_2(\lambda)b \\ & + \left(2\lambda^2 - \lambda^4 J_2(\lambda)\right)a^2 + \left(1 - \lambda^2 J_2(\lambda)\right)b^2 \\ & + \left(2\lambda - \lambda^3 J_2(\lambda)\right)ab. \end{aligned} \tag{25}$$

Let convergence factor λ in the above formula take different values:

$$\lambda = \begin{bmatrix} \lambda_1 \\ \lambda_2 \\ \lambda_3 \\ \cdots \\ \lambda_n \end{bmatrix}. \tag{26}$$

Transform the (24) as follows, and use a matrix to express the following formula:

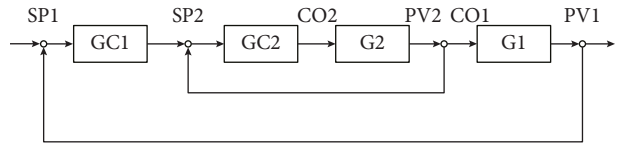

Figure 3: Cascade control system. The control block diagram of the cascading system consists of two loops, the internal and external loop.

$$Bx = J_2. \tag{27}$$

The matrix B corresponds to the coefficient matrix of (27), as follows:

$$B = \begin{bmatrix} -2\lambda_1^2 J_2(\lambda_1) - 2 & -2\lambda_1 J_2(\lambda_1) & 2\lambda_1^2 - \lambda_1^4 J_2(\lambda_1) & 1 - \lambda_1^2 J_2(\lambda_1) & 2\lambda_1 - \lambda_1^3 J_2(\lambda_1) \\ -2\lambda_2^2 J_2(\lambda_2) - 2 & -2\lambda_2 J_2(\lambda_2) & 2\lambda_2^2 - \lambda_2^4 J_2(\lambda_2) & 1 - \lambda_2^2 J_2(\lambda_2) & 2\lambda_2 - \lambda_2^3 J_2(\lambda_2) \\ \cdots & \cdots & \cdots & \cdots & \cdots \\ -2\lambda_n^2 J_2(\lambda_n) - 2 & -2\lambda_n J_2(\lambda_n) & 2\lambda_n^2 - \lambda_n^4 J_2(\lambda_n) & 1 - \lambda_n^2 J_2(\lambda_n) & 2\lambda_n - \lambda_n^3 J_2(\lambda_n) \end{bmatrix}. \tag{28}$$

The matrix J_2 corresponds to the value obtained by taking different λ values:

$$J_2 = \begin{bmatrix} J_2(\lambda_1) \\ J_2(\lambda_2) \\ J_2(\lambda_3) \\ \cdots \\ J_2(\lambda_n) \end{bmatrix}. \tag{29}$$

Unknown parameter matrix x:

$$\begin{aligned} x &= \begin{bmatrix} x_1 \\ x_2 \\ x_3 \\ x_4 \\ x_5 \end{bmatrix} \\ &= \begin{bmatrix} a \\ b \\ a^2 \\ b^2 \\ ab \end{bmatrix}. \end{aligned} \tag{30}$$

This paper uses the least-squares method to solve the value of a, b:

$$x = \left(B^{\mathrm{T}} \cdot B\right)^{-1} \cdot B^{\mathrm{T}} \cdot J_2. \tag{31}$$

According to the above model, the parameters can be solved:

$$\begin{bmatrix} x_1 \\ x_2 \end{bmatrix} = \begin{bmatrix} a \\ b \end{bmatrix}. \tag{32}$$

Incorporating the unknown parameter values, we get

$$L = -\frac{2a\lambda + b}{a\lambda^2 + b\lambda + 1} - J_1(\lambda), \tag{33}$$

$$q = G(\lambda)\left(a\lambda^2 + b\lambda + 1\right)\mathrm{e}^{-\lambda L}. \tag{34}$$

After many simulation experiments, it is found that the value of λ is preferably $\lambda = 0.16 + 0.009n$ and n is between 5 and 15. The results show that after the parameters of the second-order model with lag in (13) are returned, there is a better identification effect.

4. Simulation

In order to verify the robustness and accuracy of the identification method, simulation experiments were performed on the two systems, respectively, and the verification was verified by observing the target object model, the Nyquist curve, and the error value of the identification model of each method. In addition, a horizontal comparison between the results of the method and the results of the traditional first-order identification algorithm is used to verify the accuracy of the method. Interference noise is added to the input and output signals to verify its anti-interference ability and robustness. The concept of signal-to-noise ratio (SNR) is introduced here, and the general noise intensity is expressed by

$$NSR = \frac{\mathrm{mean}\left(abs\left(\mathrm{noise}\right)\right)}{\mathrm{mean}\left(abs\left(\mathrm{signal}\right)\right)}. \tag{35}$$

NSR is the ratio of the average of the absolute values of all noise signals to the average of the absolute values of the true signals. The SNR algorithm is expressed as

$$SNR = 20\ln\left(\frac{1}{NSR}\right)(dB). \tag{36}$$

In order to show the accuracy of the identification model more intuitively, an error algorithm is introduced to evaluate the accuracy of the model. The algorithm of ε is shown in

$$\varepsilon = \frac{1}{N}\sum_{k=1}^{N}\left[\widehat{y}(kT) - y(kT)\right]^2. \tag{37}$$

Among them, N represents the sampling time of the step response output data; T represents the sampling time; $\widehat{y}(kT)$ represents the output value of the k-th sampling point of the identification model; and $y(kT)$ represents the k-th sampling point of the original model output value.

4.1. Non-Minimum Phase System Experiment. In this section, build a simulation model for the non-minimum phase system as shown in Figure 4.

For this model, the specific model is shown in

$$G(s) = \frac{-3s+2}{2s^2+3s+1}e^{-5s}. \tag{38}$$

Using the frequency-domain identification method in this article, under the noise interference of $NSR = 20\%$, the important frequency range obtained by data analysis is between 0 and 0.3450, and 30 sample data points are also taken in this interval, and the final object model is determined by fitting these data points as (39), and the final object model is compared with the results of the traditional methods

$$G(s) = \frac{-s+0.6667}{0.6667s^2+s+0.3333}e^{-5s}. \tag{39}$$

The traditional method identification model is

$$G(s) = \frac{1.992}{11.5512s^2+4.7563s+1}e^{-3s}. \tag{40}$$

The simulation results of the models are compared intuitively in the form of pictures as shown in Figure 5 and Table 1. It can be seen from Figure 5 that the curve obtained by the method in this paper can well fit the curve of the original plant. The curve obtained by the traditional method is not very ideal.

It can be seen that the method in this paper is not weaker than the traditional method from the comparison of the Nyquist curves in Figure 6.

Figure 7 shows the results of the simulation mode of Figure 4, where the three parameters of the PID are $k_p = 0.2186$, $k_i = 0.0423$, and $k_d = -0.6026$.

4.2. Industrial Cascade System Experiment. Similar to the previous section, we should build a simulation model for the cascade system as shown in Figure 8.

This model uses the industrial steam boiler object as the object model. The specific model is shown in (41) and (42).

$$G(s) = \frac{8}{225s^2+30s+1}, \tag{41}$$

$$G(s) = \frac{1.125}{(15s+1)^3}. \tag{42}$$

The identification results of the method in this paper are as follows: the internal ring model is shown in equation (43) and the external ring model is shown in (44):

$$G(s) = \frac{8.0003}{223.9861s^2+30.7805s+1}e^{-0.2564s}, \tag{43}$$

$$G(s) = \frac{1.1204}{1050.7864s^2+60.6804s+1}e^{-10.0234s}. \tag{44}$$

Using the experimental data collected in the simulation experiment obtained, the internal and external loop models are identified by using the traditional method and the method in this paper, respectively.

The results of the traditional method are as follows. The internal loop model is shown in equation (45) and the external loop model is shown in (46):

$$G(s) = \frac{7.9795}{236.459s^2+31.0928s+1}e^{-0.2891s}, \tag{45}$$

$$G(s) = \frac{1.3085}{633.277s^2+51.095s+1}e^{-0.6346s}. \tag{46}$$

It can be seen intuitively from the last two columns of Table 2 that the direct error value between the recognition model and the target model is less than 10e-04, which is 2 orders of magnitude smaller than the error value recognized by the traditional method, which shows the accuracy of the recognition model of this method. The performance indicates that the method has high accuracy in identifying the model.

It can be seen from Figures 9(a) and 9(b) that the curve of internal loop and external loop obtained by the method in this paper can well fit the curve of the original plant. The curve obtained by the traditional method is not very ideal.

It can be seen that the method in this paper is better than the traditional method from the comparison of the Nyquist curves in Figure 10.

Figure 11 shows the results of the simulation mode of Figure 8, where the three parameters of the internal PID are $k_p = 0.0603$, $k_i = 4.5275$, and $k_d = -4.2519$, and the three parameters of the external PID are $k_p = 3.8293$, $k_i = 0.0206$, and $k_d = -834.1573$. The selection of the control method and the tuning of the control parameters will be presented in the following work.

From the last two columns in Table 2 and Figure 10, it can be seen intuitively that the direct error value between the identification model and the target model is less than $10e-04$, which is two orders of magnitude smaller than the error value identified by the traditional method. Order of magnitude, which shows the high accuracy of the identification model of this method, shows the high accuracy of the identification model of this method.

The mean square error (MSE) of internal loop transfer function and external loop transfer function obtained by this method is compared with other studies [3, 33, 34] as shown in Table 3. It is clear that the proposed CMP approach outperformed the other algorithms and has the least MSE value. The algorithm CMP (closed-loop moment parameter identification) in this paper only needs to obtain the normal operating data of the system setting value change once, which means that the algorithm may lead to overfitting. There are many studies [35–37]

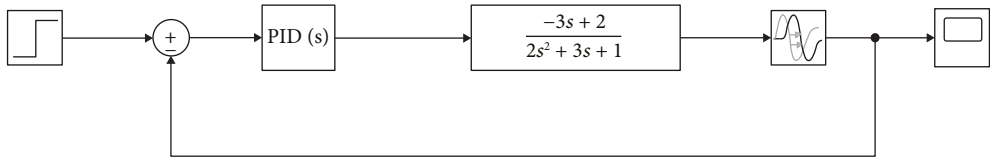

Figure 4: The simulation mode of non-minimum phase system.

Table 1: Model of non-minimum phase system error value between the identification model and the target model.

Object model	Method of this article	Error	Error for traditional method
$G(s) = (-3s + 2/2s^2 + 3s + 1)e^{-5s}$	$G(s) = (-s + 0.6667/0.6667\,s^2 + s + 0.3333)e^{-5s}$	$1.2178e-08$	$1.3e-03$

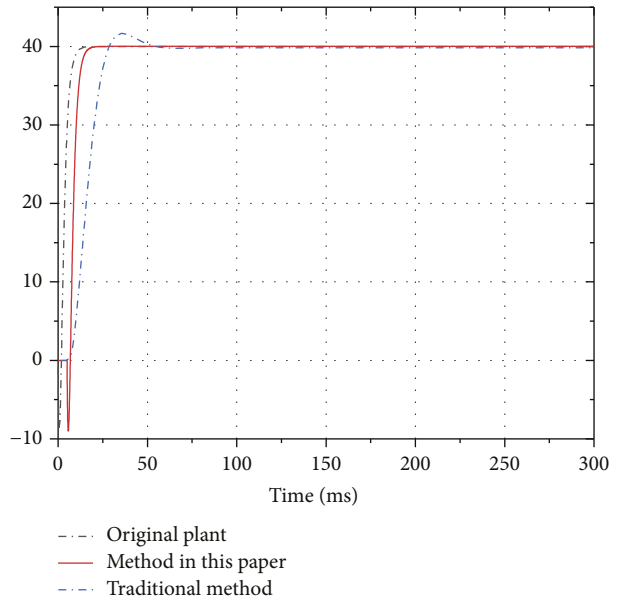

Figure 5: Comparison of the response curves of the three functions. The system identification of the original plant signal is done by the traditional method and the method of this paper, respectively.

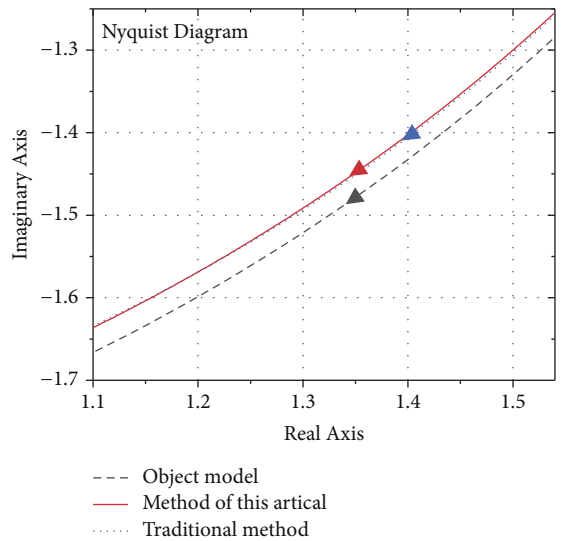

Figure 6: Comparison of Nyquist curves. These are the Nyquist curves of the transfer function identified by the method of this paper and the traditional method.

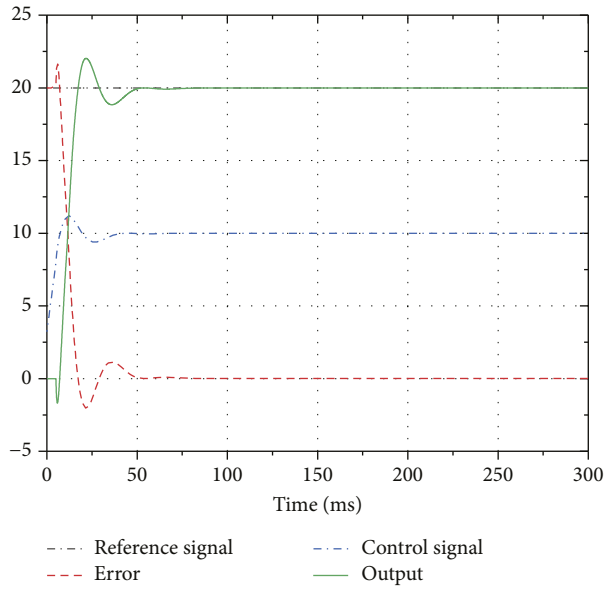

Figure 7: The simulation result of non-minimum phase system.

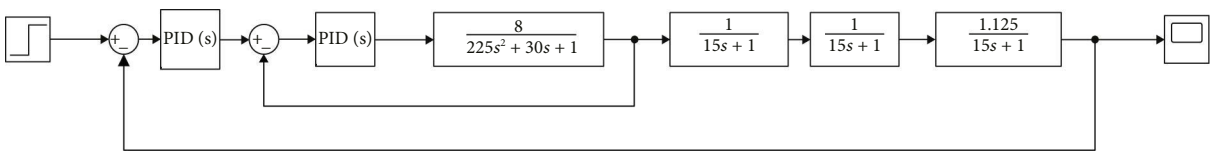

Figure 8: The simulation of the cascade system.

Table 2: Model of industrial cascade system experiment error value between the identification model and the target model.

Cascade system	Object model	Method of this article	Error	Error for traditional method
Internal loop	$G(s) = (8/225s^2 + 30s + 1)$	$G(s) = (8.0003/223.9861\,s^2 + 30.7805\,s + 1)e^{-0.2564\,s}$	$5.7534e-07$	1.2752
External loop	$G(s) = (1.125/(15s + 1)^3)$	$G(s) = (1.1204/1050.7864\,s^2 + 60.6804\,s + 1)e^{-10.0234\,s}$	$2.5913e-04$	0.2377

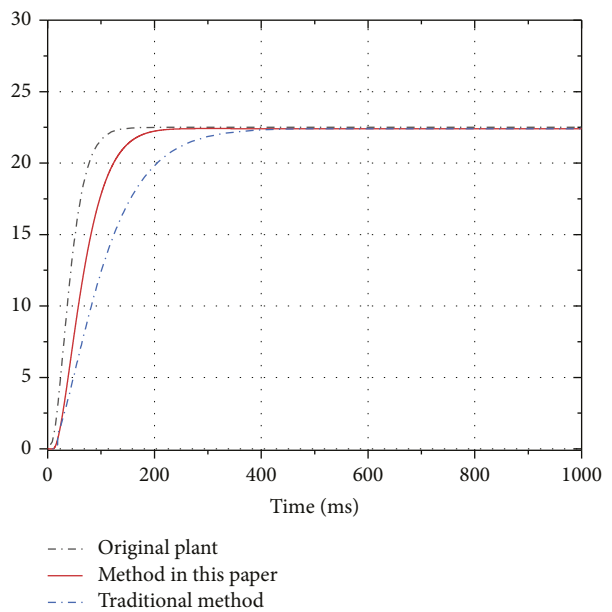

(a)

Figure 9: Continued.

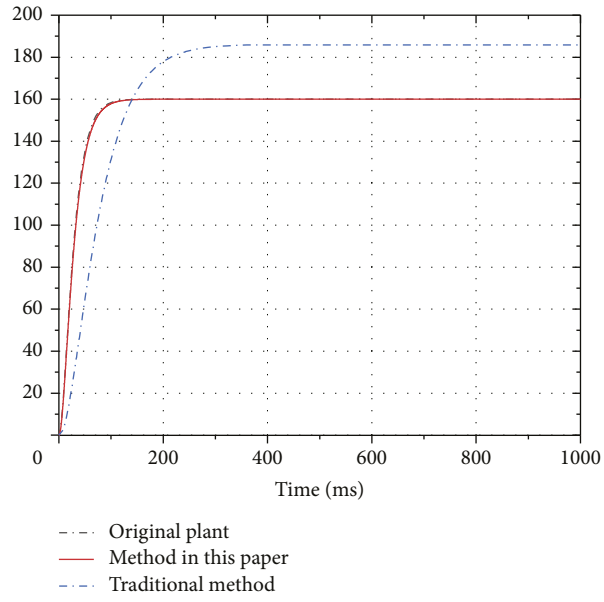

(b)

Figure 9: Comparison of the response curves of the three functions. (a) The internal loop model. (b) The external loop model. This is a comparison of the system response curves of the original plant signal, the transfer function identified by the method in this paper, and the conventional method.

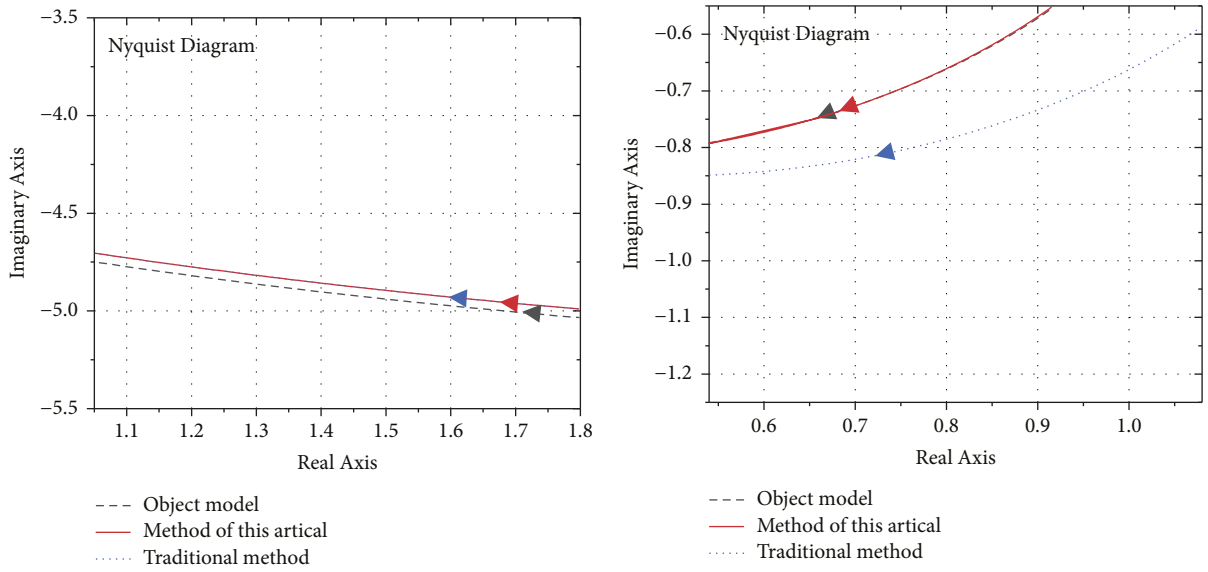

(a) (b)

Figure 10: Comparison of Nyquist curves of the internal and external loop model. (a) The internal loop model. (b) The external loop model. This is a comparison of Nyquist curves of the original plant signal, the transfer function identified by the method in this paper, and the conventional method.

devoted to solving the problem of overfitting. In Section 3, two experiments were performed on the two systems, respectively. Interference noise is added to the input and output signals to verify its anti-interference ability and robustness. Tables 1 and 2 show the noise results, which show that the algorithm is insensitive to noise in system identification. In the future, we will continue to study online system identification, and under the framework of

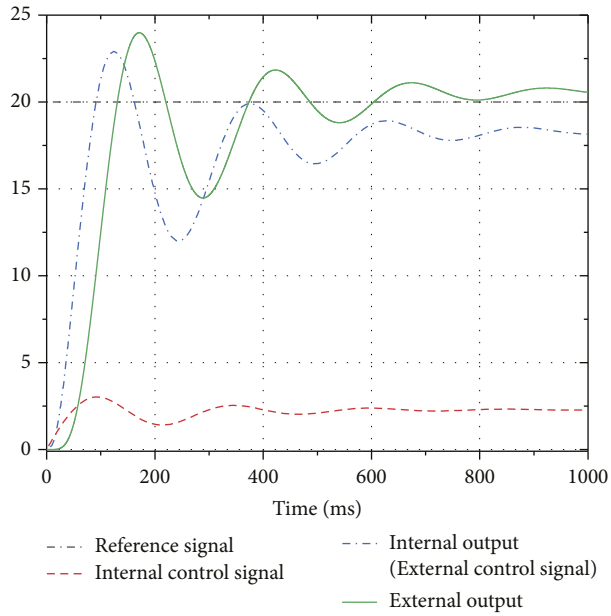

Figure 11: The simulation result of the cascade system. It shows the control signal and output signal of the inner loop and the output signal of the external loop, in which the output signal of the inner loop is the input signal of the external loop.

Table 3: A comparison of MSE results of step response using different approaches.

Method	MSE result
PNLSS-I (polynomial non-linear state space)	0.4498
NLSS2	0.3433
BLA (best linear approximation)	0.7574
Volterra models (3rd degree) (transient removal)	0.5400
Volterra models (3rd degree) (no transient est.)	2.0800
HBJ	0.0087
Proposed CMP (closed-loop moment parameter identification)	0.0049

the existing online system identification method presented in this paper, we will improve the method to achieve more ideal results and finally apply it to engineering practice.

5. Conclusion

This paper presents a model parameter identification method for an industrial cascade system. The method does not require any a priori condition and only needs to obtain the input and output data under the step response to identify the controlled objects, without complicated algorithm processing and a large number of calculations. Simulations are performed for several representative controlled objects, and the simulation results show that the method identifies the model with high accuracy and strong anti-interference capability. Even in the case that the signal-to-noise ratio is 20%, the recognition can be completed well, and the recognition accuracy is very high, which is better than some traditional recognition methods. The higher the accuracy of the identified model of the controlled object is, the better it is for the analysis of the controlled system and the parameter setting of the controller, which facilitates the whole control system to achieve a good control effect and can be used to identify the actual industrial process object.

Data Availability

The Matlab code and Simulink data used to support the findings of this study have been deposited in the GitHub repository (https://github.com/ericddm/CascadeSystemIdentification-CMP).

Conflicts of Interest

The authors declare that there are no conflicts of interest regarding the publication of this paper.

Acknowledgments

This study was supported by the National Key Research and Development Program of China (no. 2020YFC2007500).

References

[1] A. Arif, Z. Wang, J. Wang, B. Mather, H. Bashualdo, and D. Zhao, "Load modeling—a review," *IEEE Transactions on Smart Grid*, vol. 9, no. 6, pp. 5986–5999, 2018.

[2] S. L. Podvalny and E. M. Vasiljev, "Cascade identification of nonlinear systems," *Journal de Physique: Conf. Ser.*vol. 1203, Article ID 012057, 2019.

[3] I. A. Aljamaan, M. M. Al-Dhaifallah, D. T. Westwick, and D. T. Westwick, "Hammerstein box-Jenkins system identification of the cascaded tanks benchmark system," *Mathematical Problems in Engineering*, vol. 2021, Article ID 6613425, 8 pages, 2021.

[4] Q. Zhang, Ya-G. Wang, F.-F. Lee, W. Zhang, and Q. Chen, "Performance assessment of cascade control system with non-Gaussian disturbance based on minimum entropy," *Symmetry*, vol. 11, no. 3, p. 379, 2019.

[5] V. K. Cao and H. P. H. Anh, "Cascade training multilayer fuzzy model for identifying nonlinear MIMO system," *International Conference on Advances in Computational Mechanics*, pp. 1017–1031, 2017.

[6] B. Mavkov, M. Forgione, and D. Piga, "Integrated neural networks for nonlinear continuous-time system identification," *IEEE Control Syst. Lett.*vol. 4, pp. 851–856, 2020.

[7] C. V. Kien, H. P. H. Anh, N. T. Nam, and N. T. Nam, "Cascade training multilayer fuzzy model for nonlinear uncertain system identification optimized by differential evolution algorithm," *International Journal of Fuzzy Systems*, vol. 20, no. 5, pp. 1671–1684, 2018.

[8] M. M. Khorasani and E. Weyer, "Towards finite sample networked system identification: a cascade network example," in *Proceedings of the 2020 59th IEEE Conference on Decision and Control (CDC)*, pp. 306–311, IEEE, Jeju, Korea, December 2020.

[9] J. Vörös, "Recursive identification of time-varying non-linear cascade systems with static input and dynamic output nonlinearities," *Transactions of the Institute of Measurement and Control*, vol. 40, no. 3, pp. 896–902, 2018.

[10] P. Mattsson, D. Zachariah, and P. Stoica, "Identification of cascade water tanks using a PWARX model," *Mechanical Systems and Signal Processing*, vol. 106, pp. 40–48, 2018.

[11] P. S. Pal, K. Mattoo, R. Kar, D. Mandal, and S. P. Ghoshal, "Identification of wiener-hammerstein cascaded system using hybrid backtracking Search algorithm with wavelet mutation," in *Proceedings of the 2019 First International Symposium on Instrumentation, Control, Artificial Intelligence, and Robotics (ICA-SYMP)*, pp. 49–52, IEEE, Bangkok, Thailand, January 2019.

[12] D. S. Karachalios, I. V. Gosea, and A. C. Antoulas, "The Loewner framework for nonlinear identification and reduction of Hammerstein cascaded dynamical systems," *Proceedings in Applied Mathematics and Mechanics*, vol. 20, no. 1, Article ID e202000337, 2021.

[13] J. Vörös, "Modelling and identification of nonlinear cascade systems with backlash input and static output nonlinearities," *Mathematical and Computer Modelling of Dynamical Systems*, vol. 24, no. 6, pp. 593–609, 2018.

[14] H.-B. Kuntze, A. Jacubasch, J. Richalet, and C. Arber, "On the predictive functional control of an elastic industrial robot," in *Proceedings of the 1986 25th IEEE Conference on Decision and Control*, pp. 1877–1881, IEEE, Athens, Greece, December 1986.

[15] C. Huang, Y. Bai, and Y. Zhu, "PID controller design for a class of networked cascade control systems," in *Proceedings of the 2010 2nd International Conference on Advanced Computer Control*, pp. 43–47, IEEE, Shenyang, China, March 2010.

[16] K. L. Fang, *Process Control and Matlab Programming*, Publishing House of electronics industry, Beijing, China, 2nd ed edition, 2013.

[17] L. Xu, L. Chen, and W. Xiong, "Parameter estimation and controller design for dynamic systems from the step responses based on the Newton iteration," *Nonlinear Dynamics*, vol. 79, no. 3, pp. 2155–2163, 2015.

[18] S. Ahmed, "Identification from step response–The integral equation approach," *Canadian Journal of Chemical Engineering*, vol. 94, no. 12, pp. 2243–2256, 2016.

[19] C. Cox, J. Tindle, and K. Burn, "A comparison of software-based approaches to identifying FOPDT and SOPDT model parameters from process step response data," *Applied Mathematical Modelling*, vol. 40, no. 1, pp. 100–114, 2016.

[20] L. Zhou, S. Fei, and J. Huang, "Simulation study of a main stream temperature system based on predictive functional-PID Cascade Control," in *Proceedings of the 32nd Chinese Control Conference*, pp. 4083–4086, IEEE, Xi'an, China, July 2013.

[21] T. Kinoshita and T. Yamamoto, "Design and experimental evaluation of a data-oriented cascade control system," in *Proceedings of the 2017 56th Annual Conference of the Society of Instrument and Control Engineers of Japan (SICE)*, pp. 240–243, IEEE, Kanazawa, Japan, September 2017.

[22] Biyanto, T. Ruki, M. S. Alfarisi, N. Afdanny, H. Setiawan, and A. Hasan, "Simultaneous optimization of tuning PID cascade control system using Duelist Algorithms," in *Proceedings of the 2016 International Seminar on Intelligent Technology and its Applications (ISITIA)*, pp. 601–606, IEEE, Lombok, Indonesia, July 2016.

[23] Z. Xiao, S. Shan, and L. Cheng, "Identification of cascade dynamic nonlinear systems: a bargaining-game-theory-based approach," *IEEE Transactions on Signal Processing*, vol. 66, no. 17, pp. 4657–4669, 2018.

[24] F. An, Q. Wu, and B. Liu, "Audio compensation with cascade Biquad filters for feedback active noise control headphones," *Processes*, vol. 10, no. 4, p. 730, 2022.

[25] H. Jianwang, R. A. Ramirez-Mendoza, T. Xiaojun, and T. Xiaojun, "Direct data-driven control for cascade control system," *Mathematical Problems in Engineering*, vol. 2021, pp. 2021–11, 2021.

[26] C. Xu and Y. Wang, "A closed-loop frequency domain identification algorithm for non-minimum phase systems," *Information and Control*, vol. 50, pp. 435–440, 2021.

[27] F. Li, H. Lin, and D. Gao, "Direct identification method and application of common continuous model in process control," *Control Engineering*, vol. 13, pp. 310–313, 2006.

[28] T. Liu and F. Gao, *Industrial Process Identification and Control Design: Step-Test and relay-experiment-based Methods*, Springer Science & Business Media, Berlin, Germany, 1st ed edition, 2011.

[29] Q.-G. Wang, X. Guo, and Y. Zhang, "Direct identification of continuous time delay systems from step responses," *Journal of Process Control*, vol. 11, no. 5, pp. 531–542, 2001.

[30] B. Lukić, K. Jovanović, and T. B. Šekara, "Cascade gain scheduling control of antagonistic actuators based on system identification," *Advances in Service and Industrial Robotics*, pp. 425–435, 2018.

[31] N. Vega, P. Parra, L. Córdova, J. Andramuño, and J. Álvarez, "Cascade control algorithm developed with embedded systems," in *Proceedings of the 2018 IEEE International Conference on Automation/XXIII Congress of the Chilean Association of Automatic Control (ICA-ACCA)*, vol. 1–6, Concepcion, Chile, October 2018.

[32] C. Zhai, G. Xiao, M. Meng, H. Zhang, and B. Li, "Identification of catastrophic cascading failures in protected power grids using optimal control," *Journal of Energy Engineering*, vol. 147, no. 1, Article ID 06020001, 2021.

[33] R. Relan, K. Tiels, A. Marconato, and J. Schoukens, "An unstructured flexible nonlinear model for the cascaded water-tanks benchmark," *IFAC-PapersOnLine*, vol. 50, no. 1, pp. 452–457, 2017.

[34] G. Birpoutsoukis, P. Zoltán Csurcsia, and J. Schoukens, "Nonparametric Volterra series estimate of the cascaded water tanks using multidimensional regularization," *IFAC-PapersOnLine*, vol. 50, no. 1, pp. 476–481, 2017.

[35] A. Makarova, H. Shen, V. Perrone et al., "Automatic termination for hyperparameter optimization," 2022, https://arxiv.org/abs/2104.08166.

[36] H. Kim, W. Lee, and J. Lee, "Understanding catastrophic overfitting in single-step adversarial training," *Proceedings of the AAAI Conference on Artificial Intelligence*, vol. 35, no. 9, pp. 8119–8127, 2021.

[37] G. K. Gupta and D. K. Sharma, "A review of overfitting solutions in smart depression detection models," in *Proceedings of the 2022 9th International Conference on Computing for Sustainable Global Development (INDIACom)*, pp. 145–151, IEEE, New Delhi, India, March 2022.